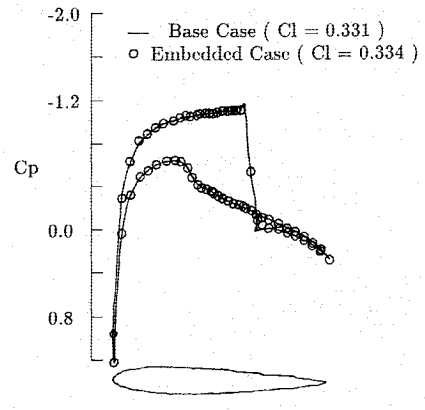

Fig. 2 Pressure distribution on the NACA 0012 airfoil, $M = 0.8$, $\alpha = 1.25$ deg.

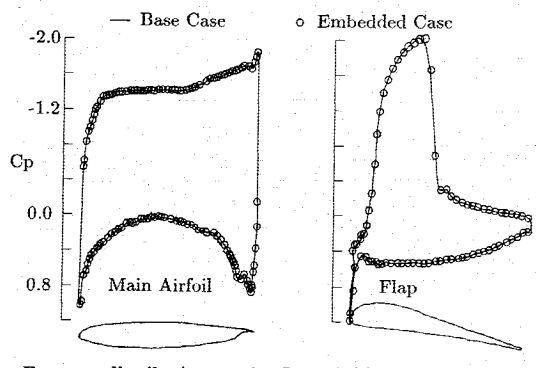

Fig. 3 Pressure distribution on the flapped SKF1.1 airfoil, $M = 0.76$, $\alpha = 3$ deg.

The base grid (no embedding) consists of 93 × 79 mesh cells. When embedding is employed, a global grid of 63 × 47 cells is used. Within this grid, a 59 × 51 cell fine grid is embedded. As shown in Fig. 1, which is drawn to scale, the interface is placed about 0.5–0.6 chords from the body. Although all global grid cells require memory allocation, only those cells outside the embedded region are computed. At certain interface locations for this grid, the refinement ratio is 4 to 1. Ratios of 3 to 1 and 2 to 1 also appear. Because the lift coefficient depends on the location of the outer boundaries,[9] calculations are carried out with outer boundary extents in all directions at 5 chords and then 10 chords. Extrapolation, as in Ref. 9, is then used to eliminate the dependence of lift coefficient C_l on boundary extent. Both grids predict about the same value of C_l when the effects of grid extent are removed (0.331 for the base grid vs 0.334 for the embedded grid). Figure 2 shows a comparison of pressure coefficient C_p distribution for the two grids when the outer boundary is placed at 10 chords. For this case, embedding results in a 21% reduction in memory requirements and a 60% reduction in CPU time.

The sensitivity of the above results to the location of the interface is discussed next. The interface for the above NACA 0012 case was placed 23% closer to the airfoil surface, i.e., to $y/c = 0.39$ where c is the chord length. The resulting change in C_l and convergence rate was less than 1%. This contrasts with the findings of Allmaras and Barron[5] which suggest that when the interface intersects a shock, small modifications in interface location produce large effects on convergence and accuracy.

An advantage of Cartesian grids is the ease with which they handle complex geometries. To illustrate this diversity, the flapped SKF1.1 airfoil is considered. Calculations are presented for the case of Mach number 0.76 and 3 deg angle of attack. The base grid is 166 × 101. The embedded grid consists of a global grid of 56 × 45 cells within which is embedded a 144 × 81 cell fine grid. The refinement ratios vary as high as 8 to 1. The extent of the outer boundary is 10 chords. Figure 3 compares C_p distributions for the main airfoil on the base grid ($C_l = 1.66$) and the embedded grid ($C_l = 1.64$). For this case, embedding results in 15% savings in memory and 45% savings in CPU time. As in the NACA 0012 case discussed earlier, the interface intersects the shock. Again, this arrangement does not introduce any problems in convergence or solution accuracy.

In conclusion, a robust embedding scheme which allows arbitrary refinement is developed for cell-centered finite volume formulations. When used in conjunction with the Runge-Kutta time stepping scheme and Cartesian grids, the scheme results in significant reduction in memory and computation time requirements without loss of accuracy.

Acknowledgments

This work was supported in part by NASA Cooperative Agreement NCCI-22.

References

[1]Clarke, D. K., Salas, M. D., and Hassan, H. A., "Euler Calculations for Multi-Element Airfoils Using Cartesian Grids," *AIAA Journal*, Vol. 24, March 1986, pp. 353–358.

[2]Gaffney, R. L., Jr., Salas, M. D., and Hassan, H. A., "Euler Calculations for Wings Using Cartesian Grids," AIAA Paper 87-0356, Jan. 1987.

[3]Usab, W. J. and Murman, E. M., "Embedded Mesh Solutions of the Euler Equations Using a Multiple Grid Method," *Proceedings of the AIAA Computational Fluid Dynamic Conference*, Danvers, MA, AIAA Paper 83-1946, July 1983.

[4]Berger, M. J. and Jameson, A., "Automatic Adaptive Grid Refinement for the Euler Equations," *AIAA Journal*, Vol. 23, No. 4, April 1985, pp. 561–568.

[5]Allmaras, S. R. and Barron, J. R., "Embedded Mesh Solutions of the 2-D Euler Equations: Evaluation of Interface Formulations," AIAA Paper 86-0509, Jan. 1986.

[6]Jameson, A., Schmidt, W., and Turkel, E., "Numerical Solution of the Euler Equations by Finite Volume Methods Using Runge-Kutta Time Stepping Schemes," AIAA Paper 81-1259, June 1981.

[7]Jameson, A. J. and Baker, T. J., "Solution of the Euler Equations for Complex Configurations," AIAA Paper 83-1929, July 1983.

[8]Berger, M. J., "On Conservation at Grid Interfaces," ICASE Report No. 84-43, NASA Langley Research Center, Sept. 1984.

[9]Thomas, J. L. and Salas, M. D., "Far-Field Boundary Conditions for Transonic Lifting Solutions to the Euler Equations," AIAA Paper 85-0020, Jan. 1985.

Buckling Analysis of Sandwich Columns of Linearly Varying Thickness

N. Paydar*
Purdue University, Indianapolis, Indiana

Nomenclature

d = diameter of an inscribed circle in a honeycomb cell
D_o = flexural stiffness of the column at $x = 0$
E = modulus of elasticity of the face material
G' = core effective shear modulus
G_c = shear modulus of the core material
H = nondimensional measure of core thickness ($= h/h_o$)
h = core thickness
h_o = core thickness at $x = 0$
K = core geometric factor
k = critical load parameter
ℓ = length of the column

Received Nov. 20, 1986; revision received Oct. 9. 1987.

*Assistant Professor of Mechanical Engineering, School of Engineering and Technology.

M = moment per unit column width
$\bar{M}$ = dimensionless moment per unit column width
P = applied compressive load
Q = transverse shear force per unit column width
$\bar{Q}$ = dimensionless transverse shear force per unit column width
R = dimensionless measure of transverse shear flexibility ($= D_n/G'h_o\ell^2$)
s = distance coordinate measured along the face sheet, see Fig. 1
t = face thickness
t_c = honeycomb wall thickness
u_s = displacement tangent to the face-sheet surface
w = transverse deflection
$\bar{w}$ = dimensionless transverse deflection
x = coordinate along the column axis
β = taper constant
γ = core shear angle
ε_s = upper face-sheet strain
θ = cross-sectional rotation, see Fig. 2
ξ = dimensionless coordinate along column axis
σ = face sheet normal stress
τ = core shear stress
ϕ = face sheet sloping angle

Introduction

SANDWICH construction has been used in aircraft for many years. In recent years, with the advent of high performance vehicles, a new type of sandwich construction, namely full-depth honeycomb, has come to be used as primary structural components in aircraft. Often these structures are tapered for either aerodynamic limitations or further weight reduction.

In the very few papers available on sandwich construction of variable thickness, the stability of columns has not been considered. Cheng[1] considered torsion of sandwich plates of trapezoidal cross section. Gupta and Jain[2] obtained the first four normal modes of vibration of annular sandwich plates of linearly varying thickness. Huang and Alspaugh[3] considered minimum-weight sandwich beam design using the governing equations of constant-thickness sandwich beam theory, but allowing the beam stiffness to be functions of the core thickness. Paydar and Libove[4] developed a theory for stress analysis of sandwich plates of variable thickness. It was shown that the use of constant thickness sandwich plate theory can lead to significant errors if it is applied to sandwich plates of variable thickness.

Buckling analysis of sandwich columns of linearly varying thickness is considered in what follows here. The column under consideration is shown in Fig. 1. For simplicity, the column is assumed to be symmetric about its axis. Since the geometric symmetry is the rule in most practical cases, this assumption is not considered to be a serious limitation in the applicability of the theory presented in this paper. The face sheets are assumed to be very thin compared to the core and are treated as membranes. The core is assumed to be inextensible in the thickness direction, to carry only transverse shear stress on its vertical cross section, and to be deformable in transverse shear. Furthermore, it is assumed that the entire compressive load is carried by the two faces alone. This assumption is warranted due to the smallness of the core's modulus in the direction of the axis of the column.

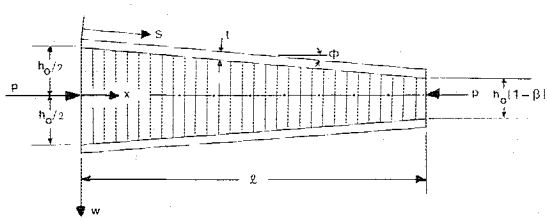

Fig. 1 Sandwich column of linearly varying thickness.

Strains and Stresses

Figure 2 shows an infinitesimal element in its deformed state. The column axis has developed lateral deflection $w(x)$ and the cross sections have undergone rotations $\theta(x)$ (positive clockwise). This figure also shows the shear angle γ. The relationship

$$\gamma = \frac{dw}{dx} - \theta$$

is apparent in the diagram. The variables w and θ impart to a point on the upper face sheet the displacement

$$u_s = \frac{h}{2}\theta\cos\phi + w\sin\phi \tag{1}$$

tangent to the face-sheet surface. As shown in Fig. 1, ϕ and s are the sloping angle and the tangential coordinate axis of the face sheet, respectively. The variable u_s gives rise to the strain

$$\varepsilon_s = \frac{du_s}{ds} = \cos\phi\frac{du_s}{dx} = \frac{h}{2}\cos^2\phi\frac{d\theta}{dx} + \frac{1}{2}\sin 2\phi\left(\frac{dw}{dx} - \theta\right) \tag{2}$$

in the upper face sheet. The corresponding strain in the lower face sheet is $-\varepsilon_s$. The face sheet stress is given by

$$\sigma = E\left[\frac{h}{2}\cos^2\phi\frac{d\theta}{dx} + \frac{1}{2}\sin 2\phi\left(\frac{dw}{dx} - \theta\right)\right] \tag{3}$$

and core shear stress is

$$\tau = G'\gamma = G'\left(\frac{dw}{dx} - \theta\right) \tag{4}$$

G' is given by the following relation for honeycomb cores[6]

$$G' = K(t_c/d)G_c$$

Equilibrium and the Stress Resultants

The stress resultants—force and moment per unit column width—shown in Fig. 2 are related to the stresses carried by the face sheets and the core as

$$Q = \tau h + 2\sigma t\sin\phi \tag{5}$$

$$M = -\sigma\tau h\cos\phi \tag{6}$$

The first term in the right-hand side of Eq. (5) is the shear carried by the core, and the second term represents the contribution of the transverse component of the face sheet stress to the total shear carried by the column.

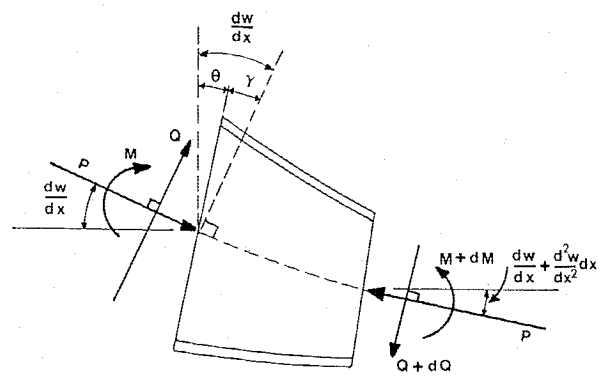

Fig. 2 Deformed element.

Substitution of Eqs. (3) and (4) into Eqs. (5) and (6), and upon nondimensionalization, yields the following relations

$$\bar{Q} = \frac{H}{R}\left(\frac{dw}{d\xi} - \theta\right) - 2\bar{M}\frac{\ell}{h_o}\frac{\tan\phi}{H} \tag{7}$$

$$\bar{M} = -H^2\cos^3\phi\left[\frac{d\theta}{d\xi} + 2\frac{\ell}{h_o}\frac{\tan\phi}{H}\left(\frac{d\bar{w}}{d\xi} - \theta\right)\right] \tag{8}$$

where $\xi = x/\ell$, $H = h/h_o$ with h_o being the column thickness at $x = 0$; for linear thickness variation $H = 1 - \beta\xi$, where β is the column taper constant. The nondimensional stress resultants are defined as

$$\bar{M} = \frac{M\ell}{D_o} \quad \bar{Q} = \frac{Q\ell^2}{D_o}$$

where $D_o(= Eth_o^2/2)$ is the column bending stiffness at $x = 0$; $\bar{w}$ is the nondimensional deflection and is defined as $\bar{w} = w/\ell$. The parameter R is defined as $R = D_o/(G'h_o\ell^2)$ and represents the ratio of flexural stiffness to transverse shear stiffness. The amount of shear deformation in the column is controlled by value of R. For example, $R = 0$ corresponds to a column with infinite shear stiffness; thus, no shear deformation is allowed in this column.

Equilibrium of vertical forces and moments for the deformation elements of Fig. 2 dictates the following nondimensional relationships:

$$\bar{Q} = \frac{d\bar{M}}{d\xi} \tag{9}$$

$$\frac{d\bar{Q}}{d\xi} = k^2\frac{d^2\bar{w}}{d\xi^2} \tag{10}$$

where

$$k^2 = \frac{P\ell^2}{D_o}$$

Equations (7–10) are the basic differential equations of variable thickness symmetric sandwich columns. The critical load of such columns can be determined from Eqs. (7–10) subject to proper boundary conditions.

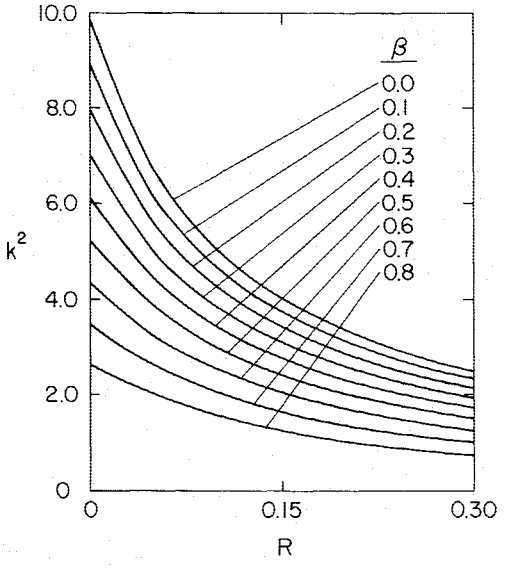

Fig. 3 Variation of buckling load parameter k^2 of simply supported variable thickness columns.

End Conditions

The mathematical description of three common types of boundary conditions will be given in this section. The conditions at a hinged end, i.e., an end cross section prevented from deflecting but free to rotate, are described by the equations $\bar{w} = 0$ and $\bar{M} = 0$. The boundary conditions associated with built-in end are $\bar{w} = 0$ and $\theta = 0$ (not $d\bar{w}/d\xi = 0$). Finally, if an end is free, except for the presence of the horizontal force P, the boundary conditions are $\bar{M} = 0$ and $\bar{Q} = k^2\, d\bar{w}/d\xi$, where the last equation results from decomposing the horizontal end force P into one component tangential to the axis and a second component (Q) perpendicular to the first.

Illustrative Application: Hinged-Hinged Column

In this section, we obtain the critical load parameter k^2 for a sandwich column of linearly varying thickness that is hinged at both ends. For this statically determinant column, the nondimensional bending moment $\bar{M}$ is given by

$$\bar{M} = k^2\bar{w} \tag{11}$$

Substitution of Eq. (11) into the governing equations (7–10) and the reduction of the resulting equations into one yields

$$\left(1 - \frac{Rk^2}{H}\right)\frac{d^2\bar{w}}{d\xi^2} - \frac{Rk^2}{H^2}\beta\frac{d\bar{w}}{d\xi} + \left[\frac{\sec^3\phi}{H^2} + \frac{4R\ell\tan\phi}{h_o^2H^3}(\ell\tan\phi - \beta h_o)\right]k^2\bar{w} = 0 \tag{12}$$

Expressing Eq. (12) in a finite difference form for grid points along the axis of the column leads to the eigenvalue problem of the form

$$[D]\{\bar{w}\} = (1/k^2)\{\bar{w}\} \tag{13}$$

Equation (13) is then used in matrix iteration procedure, namely, the sweeping technique[5] to yield the critical load and the associated eigenvector.

Figure 3 shows the variation of k^2 as a function of R for various values of column thickness taper constant, β. The reduction of k^2 at $R = 0$ (no shear deformation) for the columns in Fig. 3 is because by increasing β, the face-sheet stresses are increased, thereby increasing the bending deflection and therefore decreasing k^2. For $R \neq 0$, it is noted that k^2 decreases at a faster rate for smaller values of β than for the larger values of β. This is attributed to the fact that by increasing β (i.e., increasing the thickness taper), the participation of the face-sheet stresses in resisting transverse shear is increased, which reduces the core shear stress and therefore the deflection due to shear. Finally, for all the columns of Fig. 3, the critical load parameter k^2 decreases rapidly and then slowly with an increase of R (i.e., increase of column shear deformation). Therefore, k^2 is more sensitive to smaller values of R.

Conclusion

The governing equations for buckling analysis of variable thickness sandwich columns are presented. In this analysis, the column is assumed to be symmetric about its axis. The face sheets are treated as membranes: the core is assumed to be inextensible in the thickness direction and to be deformable in transverse shear. The theory takes into account the contribution of the fact-sheet membrane forces (by virtue of their slopes) to the transverse shear. Numerical results are presented for a column hinged at both ends with linear thickness variation.

References

[1]Cheng, S., "Torsion of Sandwich Plates of Trapezoidal Cross Section," *ASME Journal of Applied Mechanics*, Vol. 28, Sept. 1961, pp. 363–366.

[2]Gupta, A. P. and Jain, M., "Axisymmetric Vibration of Annular Sandwich Plates of Linearly Varying Thickness," *Journal of Sound and Vibration*, Vol. 80, March 1982, pp. 329–337.

[3]Huang, S. N. and Alspaugh, D. W., "Minimum Weight Design," *AIAA Journal*, Vol. 12, Dec. 1974, pp. 1617–1618.

[4]Paydar, N. and Libove, C., "Stress Analysis of Sandwich Plates with Unidirectional Thickness Variation," *ASME Journal of Applied Mechanics*, Vol. 53, Sept. 1986, pp. 609–613.

[5]Meirovitch, L., *Analytical Methods in Vibrations* (1st Ed.) Macmillan, New York, 1967, pp. 91–99.

[6]Vinsom, J. R., "Optimum Design of Composite Honeycomb Sandwich Panels Subjected to Uniaxial Compression," *AIAA Journal*, Vol. 24, Oct. 1986, pp. 1690–1696.